enabling Thomer's results to be reproduced rather faithfully suggests that it will be very worthwhile to carry this kind of approximation further, and we are now undertaking more detailed treatments of the H_2O and the NH_3 molecules, based on the results of this paper, in which angular terms will be included in the density. For H_2O we hope to make a detailed comparison of the method we are proposing with the LCAO self-consistent-field treatment (Roothaan, 1951) which has been worked out in detail for this case by Ellison & Shull (1953, see also Amako, 1954) whilst for NH_3 we hope to present calculations giving the total energy as a function of the N–H distance. A particularly interesting point in both cases will be to see whether one can calculate reasonably accurate dipole moments with only a few angular terms in the electron density. The results of these investigations will be published elsewhere at a later date.

We should like to thank Prof. C. A. Coulson, F.R.S., for a critical reading of the manuscript and Dr M. J. M. Bernal for a helpful correspondence before this investigation was undertaken. One of us (K. E. B.) wishes to acknowledge a Maintenance Grant from the Department of Scientific and Industrial Research.

References

AMAKO, Y. (1954). *Sci. Rep. Tôhoku Univ.* (1), **38**, 77.
BERGHUIS, J., HAANAPPEL, I. M., POTTERS, M., LOOP-STRA, B. O., MACGILLAVRY, C. H. & VEENENDAAL, A. L. (1955). *Acta Cryst.* **8**, 478.
BERNAL, M. J. M. (1953). *Proc. Phys. Soc.* A, **66**, 514.
BROWN, F. W. (1933). *Phys. Rev.* **44**, 214.
BUCKINGHAM, R. A., MASSEY, H. S. W. & TIBBS, S. R. (1941). *Proc. Roy. Soc.* A, **178**, 119.
DUNCANSON, W. E. & COULSON, C. A. (1944). *Proc. Roy. Soc. Edinb.* A, **62**, 37.
ELLISON, F. O. & SHULL, H. (1953). *J. Chem. Phys.* **21**, 1420.
FOCK, V. & PETRASHEN, M. J. (1934). *Phys. Z. Sowjet*, **6**, 368.
JAMES, R. W. & BRINDLEY, G. W. (1931). *Phil. Mag.* (7), **12**, 81.
McWEENY, R. (1951). *Acta Cryst.* **4**, 513.
MORSE, P. M., YOUNG, L. A. & HAURWITZ, E. S. (1935). *Phys. Rev.* **48**, 948.
MULLIKEN, R. S. (1955). *J. Amer. Chem. Soc.* **77**, 887.
PIRENNE, M. H. (1946). *The Diffraction of X-rays and Electrons by Free Molecules*. Cambridge: University Press.
ROOTHAAN, C. J. (1951). *Rev. Mod. Phys.* **23**, 69.
THOMER, G. (1937). *Phys. Z.* **38**, 48.
WOLLAN, E. O. (1931). *Phys. Rev.* **37**, 862.

Electron-Diffraction Study of the Structure of Basic Lead Carbonate, 2PbCO₃.Pb(OH)₂

By J. M. COWLEY

Chemical Physics Section, Division of Industrial Chemistry, Commonwealth Scientific and Industrial Research Organization, Box 4331, G. P. O., Melbourne, Victoria, Australia

Previously established techniques and some new techniques, including the use of modified Patterson functions and the derivation of three-dimensional Patterson functions by a 'stereoscopic' method, have been applied to the structure analysis of single crystals of basic lead carbonate by electron diffraction. The crystals have a disordered layer lattice and the structure was analysed by the 'distribution-function' method. The individual layers have a trigonal unit cell, $P31m$ with $a = b = 9·06$, $c = 8·27$ Å, and contain a $Pb(OH)_2$ sheet sandwiched between two $PbCO_3$ sheets. On the average the layers have approximate rhombohedral stacking, giving $c = 24·8$ Å, but the deviations from this are such that a fully-ordered structure would be triclinic, $P1$.

The modification of the intensities by the difference in phase of electrons scattered from light and heavy atoms is calculated, and its importance in structure analysis is assessed

Introduction

The structure of basic lead carbonate, better known as white lead, has not, as far as can be determined, previously been studied by diffraction methods. By X-ray diffraction, only powder patterns have been obtained. Because of the small crystal size of white lead, the powder patterns contain relatively few lines,

poorly defined, and do not form a suitable basis for a structure analysis.

The structure analysis based on single-crystal electron-diffraction patterns was undertaken as an exercise in the use of the techniques previously developed (Cowley, 1953a, b) and as a test for new techniques more recently devised. These include the use of a modified Patterson function (Cowley, 1956a) and the

use of tilted patterns for 'stereoscopic' three-dimensional structure analysis (Cowley, 1956b), described in accompanying articles. Because of the large difference in atomic numbers of the atoms present, the structure analysis also provided an opportunity of assessing the importance of the differences in phase shift of scattered electrons for heavy and light atoms (Glauber & Schomaker, 1953; Hoerni & Ibers, 1953). A further feature of interest was that the 'distribution-function' method of dealing with disordered structures (Cowley, 1953b) was employed more extensively than before. In all, the structure analysis demonstrates the power of the single-crystal electron-diffraction techniques in locating both heavy and light atoms in a rather large unit cell of low symmetry in a case where the crystals are too small to give useful X-ray diffraction patterns.

Electron-diffraction ring patterns of basic lead carbonate were obtained by Fordham & Tyson (1937) from the precipitate formed by adding caustic soda to lead acetate solution. The rings were attributed to a hydroxide, but it is known (see, for example, Clark & Tyler, 1939) that the hydroxide precipitates take up carbon dioxide from water or air rapidly unless special precautions are taken. The d values agreed with the A. S. T. M. *Card Index* X-ray data for the basic carbonate. They were interpreted in terms of a close-packed hexagonal cell with $a = 5\cdot26$, $c = 14\cdot7$ Å.

In the present case the crystals studied were formed by the action of water or dilute ammonium hydroxide solution on particles of lead fume, called 'lead suboxide', but shown by X-ray diffraction to be a mixture of finely divided lead and lead oxides. While observing specimens prepared from water suspensions of lead fume with an R.C.A. EMU electron microscope, Miss R. J. Beckett of this Section observed the growth of thin sheets of the basic carbonate around the lead fume particles. The sheets initially were roughly circular. With continued growth their outlines tended to become hexagonal and they contained concentric circular or near-hexagonal bands of thicker material. Fig. 1 is an electron micrograph of crystal sheets at an advanced stage of growth. The lead fume particles have completely disappeared from the centres of the sheets.

Electron-diffraction patterns were obtained with the improved form of the high-resolution electron-diffraction camera described by Cowley & Rees (1953). With the beam focused on the photographic plate, specimens prepared on collodion films gave sharp ring patterns which showed considerable arcing when the specimen was tilted. With a beam of small divergence focused on the specimen, extensive single-crystal spot patterns from individual crystals were obtained both for normal incidence, when the pattern had very nearly hexagonal symmetry, and for all angles of tilt. It was concluded that the crystals had a disordered layer-lattice structure with the layers parallel to the plane of the sheets.

Interpretation of diffraction patterns

In the ring patterns the stronger rings were similar to those observed by Fordham & Tyson (1937), but in addition a large number of closely-spaced weak rings was resolved. All observed rings could be indexed on the basis of a hexagonal unit cell with dimensions

$$a = 9\cdot06, \quad c = 24\cdot8 \text{ Å} .$$

Because of the preferred orientation and the morphology of the crystals, $00l$ reflexions could not be observed. The c-axis dimension and the indices of the hkl reflexions were checked and found consistent with the arcing of the rings in tilted patterns. The a axis was increased by a factor of $\sqrt{3}$ over that found by Fordham & Tyson by the presence of weak rings with $h - k \neq 3n$. In the hexagonally symmetric $hk0$ single-crystal spot pattern, the reflexions for which $h - k \neq 3n$ were, in general, very weak. Those with $h - k = 3n$ were stronger and, of these, reflexions for which $h = 3n$, $k = 3m$ were very strong. In tilted patterns the intensities were markedly different and the hexagonal symmetry was lost, although the tendency for $h - k = 3n$ reflexions to be stronger remained. No systematic absences were observed.

For the density of white lead, various authors have given values ranging from $6\cdot14$ to $6\cdot80$ g.cm.$^{-3}$. If the upper value is taken, calculation gives $Z = 9\cdot1$, i.e., the unit cell contains $18PbCO_3 . 9Pb(OH)_2$. The intensities of the single-crystal reflexions were found by using a microphotometer on patterns in which each spot was spread over a rectangular area by means of deflector plates. One of the tilted patterns of basic lead carbonate was used as an illustration when this method was first described (Cowley, 1953a). All spots were measured for which $h^2 + hk + k^2 \leq 100$.

Fig. 1. Electron micrograph of basic lead carbonate particles.

Effects of phase shifts

Before proceeding with the structure analysis it was necessary to assess the effect on the intensities of the phase shift which occurs when electrons are scattered by atoms (Glauber & Schomaker, 1953; Hoerni & Ibers, 1953).

The phase shift increases with the atomic weight and the scattering angle. When both heavy and light atoms are present the differences in phase shift may become important. In gas diffraction work it has been shown that the intensities at high angles of diffraction may be changed enough to lead to serious errors in molecular structure determinations. In crystal-structure analysis the maximum angles of diffraction are not so great. The intensity changes should be less marked.

In considering the phase effects in basic lead carbonate patterns, the carbon atoms may be considered as equivalent to oxygen atoms, so that only η_{Pb} and η_O, the phase shifts for lead and oxygen, need be considered. The structure factor $E = E_{hk}$ may be expressed as the sum of contributions from lead and oxygen; thus $E = E_{Pb} + E_O = (A_{Pb} + iB_{Pb}) + (A_O + iB_O)$.

Taking account of the phase shifts, the intensity is given, apart from a constant term, by

$$I_{hk} = (E_{Pb} \exp i\eta_{Pb} + E_O \exp i\eta_O)$$
$$\times (E_{Pb} \exp i\eta_{Pb} + E_O \exp i\eta_O)^*$$
$$= (E^{Pb} + E_O \exp i\Delta\eta) . (E_{Pb} + E_O \exp i\Delta\eta)^*$$
$$= (A_{Pb} + A_O \cos \Delta\eta + B_O \sin \Delta\eta)^2$$
$$+ (B_{Pb} - A_O \sin \Delta\eta + B_O \cos \Delta\eta)^2,$$

where $\Delta\eta = \eta_{Pb} - \eta_O$.

Since B_O is antisymmetric it follows that $I_{hk} \neq I_{\bar{h}\bar{k}}$ unless the structure is centrosymmetric. Hence it should be possible, in principle, to determine whether or not a structure has a centre of symmetry by examination of the intensities. In practice the combined effects of the finite radius of the Ewald sphere and slight tilts of the crystal mask any asymmetry of the intensities due to the phase effect.

The intensities of equivalent reflexions are usually averaged to give

$$\tfrac{1}{2}(I_{hk} + I_{\bar{h}\bar{k}}) = A_{Pb}^2 + B_{Pb}^2 + A_O^2 + B_O^2$$
$$+ 2(A_O A_{Pb} + B_O B_{Pb}) \cos \Delta\eta$$
$$= E . E^* - 2(A_O A_{Pb} + B_O B_{Pb})$$
$$\times (1 - \cos \Delta\eta) .$$

The value of $(1 - \cos \Delta\eta)$ in the present case exceeds 0.3 only for one or two of the outermost reflexions. Since, on the average, the values of A_O and B_O are of the order of one-fifth of those of A_{Pb} and B_{Pb} the values of $\tfrac{1}{2}(I_{hk} + I_{\bar{h}\bar{k}})$ differ very little from those expected in the absence of a phase shift. Consequently the correction to the intensities for the phase effect was neglected until the refinement stage of the structure analysis.

When the correction term was calculated on the basis of an approximate structure, it was found that the average correction to the intensities was less than 1%. The maximum correction, occurring for a weak reflexion, was 20%. Except in this case, the correction was much less than the experimental error of intensity measurement.

It would seem from this experience that, unless intensity measurements are made at considerably larger diffraction angles, the effect of the phase shift on the intensities need be considered only in cases where the total scattering power of the light atoms is of the same order as that of the heavy atoms, i.e. when there are many light atoms for each heavy atom.

In the present case, a correction was made for the phase shifts in the calculation of structure factors and phase angles in the refinement stages.

Three-dimensional modified Patterson function

Intensities were measured from two spot patterns: the $hk0$ spot pattern obtained with the beam very nearly parallel to the c axis, and a 'tilted' pattern, the tilt being $17\tfrac{1}{2}°$ about an axis very nearly parallel to the a_2 axis of the crystal lattice. Instead of normal Patterson projections, modified Patterson projections were calculated using $I_{hk} - 3I_{hk}^2 + 4I_{hk}^3 - I_{hk}^4$ as coefficients of the Fourier series, with the intensities scaled down so that the maximum intensity had a value 0.5 (Cowley, 1956a). These had the advantage of being sharpened and also of emphasizing the information contained in the values of the intensities of the weak spots with $h - k \neq 3n$.

The two modified Patterson projections were used to deduce a number of sections of the three-dimensional modified Patterson function by the 'stereoscopic' method described in an accompanying paper (Cowley, 1956b). The two projections, and the sections deduced for $z = 0$ and $z = 0.13$, are reproduced in this paper to illustrate the method.

The principal features of the 'untilted' Patterson projection are very high peaks at the origin and $\pm(\tfrac{1}{3}, \tfrac{2}{3})$ and high peaks at $\pm(\tfrac{1}{3}, 0)$, $\pm(0, \tfrac{1}{3})$, $\pm(\tfrac{1}{3}, \tfrac{1}{3})$. The peaks at $(0, 0)$ and $\pm(\tfrac{1}{3}, \tfrac{2}{3})$ are present in the sections $z = 0$, $z = \tfrac{1}{3}$, $z = \tfrac{2}{3}$ etc. The peaks at $\pm(\tfrac{1}{3}, 0)$ etc. are missing from these sections, but are present most strongly in the sections $z = \tfrac{1}{9}$, $z = \tfrac{2}{9}$, $z = \tfrac{4}{9}$ etc.

All of these high peaks may be attributed to Pb–Pb vectors. Since the unit cell contains 27 Pb atoms, and the c axis is approximately nine times the distance between planes of Pb atoms in the $PbCO_3$ structure (Colby & Lacoste, 1933), it may be concluded that the Pb atoms are arranged in nine planes with each plane containing three Pb atoms in approximately hexagonal array, e.g. at $(0, 0)$ and $\pm(\tfrac{1}{3}, \tfrac{2}{3})$. The distance between Pb atoms in a plane is then about 5.2 Å, as in $PbCO_3$.

It follows from the Patterson sections that the Pb planes are stacked with a displacement $\pm(\tfrac{1}{3}, 0)$, or the equivalent, between them, i.e. the stacking is of
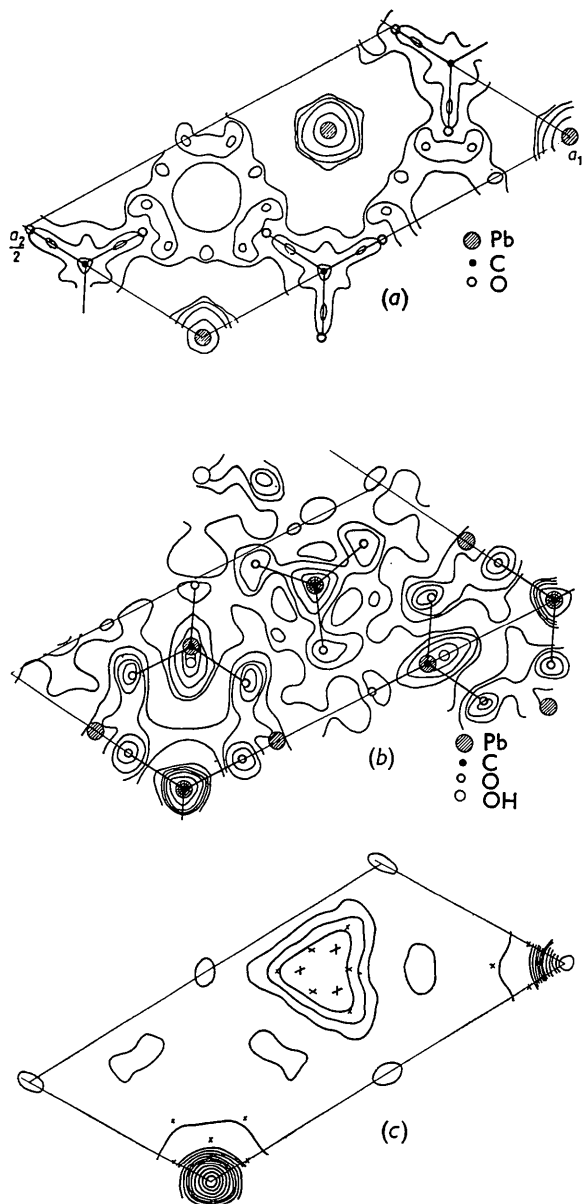
(a)

⊘ Pb
• C
○ O

(b)

⊘ Pb
• C
○ O
○ OH

(c)

Fig. 2. (a) Section of the basic lead carbonate unit cell showing a $PbCO_3$ layer, obtained by image-seeking.

(b) Final difference-Fourier projection of basic lead carbonate layer. Contributions of Pb atoms in the indicated positions have been subtracted.

(c) Final distribution-function Patterson projection for the stacking of basic lead carbonate layers. The crosses indicate the 'idealized' vector translations. A number of contours have been omitted from the origin peak.

the $A\,B\,C$ type occurring in the face-centred cubic close-packing. If the layers were all equivalent, with a hexagonal arrangement of Pb, the unit cell would have an a axis of 5·2 Å and a c axis of 8·3 Å, or one-third of the observed c axis. Since, in fact, the Patterson sections seem to recur approximately at intervals of one-third of the c axis, it may be deduced that the

structure is made up of composite layers each containing three planes of Pb atoms which are stacked approximately in an $A\,B\,C$ sequence, but which deviate from the 5·2 Å hexagonal array in such a way that the composite layer as a whole has an a axis of 9·06 Å. Three of these composite layers are contained in the unit cell. Since the only large peaks in the $z = \frac{1}{3}$ section are at (0, 0) and $\pm(\frac{1}{3}, \frac{2}{3})$, the translation between the layers must be $\pm(\frac{1}{3}, \frac{2}{3})$. Hence the stacking of the composite layers follows an $A\,B\,C$ sequence.

From the tilted single-crystal patterns it is evident that there is considerable disorder in the stacking of the layers, since the scattering power seems to be continuous along the hk lines parallel to the c^* axis. One would therefore not expect the definite indication of a 24·8 Å c axis found in the ring patterns. The explanation is that most of the crystals involved in the formation of the ring patterns were thicker and possibly better ordered than the large thin plates which gave the best spot patterns.

In view of the similarity of the arrangement of the planes of Pb atoms with that in the $PbCO_3$ structure, it seems likely that the geometric relationship of the Pb atoms and CO_3 groups would be the same in the two structures. This was confirmed by image-seeking on the Patterson sections, using the minimum function. Fig. 2(a) shows the $z = 0$ section of the unit cell obtained by image-seeking with the points (0, 0, 0), $(\frac{1}{3}, \frac{2}{3}, 0)$, $(\frac{2}{3}, \frac{1}{3}, 0)$, $(-\frac{1}{3}, 0, 0.13)$, $(0, -\frac{1}{3}, 0.13)$ and $(\frac{1}{3}, \frac{1}{3}, 0.13)$. The occurrence of three CO_3 groups around each Pb atom is clearly confirmed. The fact that each C and O position is surrounded by a group of three small peaks may result because the Pb atoms on the $z = 0.13$ plane are not exactly at the $(-\frac{1}{3}, 0)$, $(0, -\frac{1}{3})$ and $(\frac{1}{3}, \frac{1}{3})$ positions.

The composite layers may therefore be considered as made up of $2PbCO_3$ layers with one $Pb(OH)_2$ layer probably sandwiched between them.

Use of a distribution-function Patterson projection

The disordered nature of the structure suggested that the best method of structure analysis would be to use the distribution-function method previously used in the study of boric acid (Cowley, 1953b). In the present case the approach was different since the nature of the distribution function could be deduced from the Patterson function, but the layer structure was unknown, whereas for boric acid the layer structure was fairly well known and the distribution function was unknown.

As a first step a distribution-function Patterson projection, $Q(x, y)$ was proposed, assuming an $A\,B\,C$-type layer stacking with a decrease in the coherence of more distant layers due to finite crystal thickness or the presence of occasional random translations between layers, i.e. $Q(x, y)$ was assumed to consist of a large peak at the origin and smaller peaks at $\pm(\frac{1}{3}, \frac{2}{3})$. The ratio of peak heights was deduced from the

relative heights of corresponding peaks in the normal Patterson function, $P(x, y, z)$. The intensities corresponding to a single layer, I_{hk}^0, were then found from the relation

$$I_{hk} = C_{hk}^2 \cdot I_{hk}^0 ,$$

where the C_{hk}^2 are the Fourier coefficients of $Q(x, y)$ and the I_{hk} are the intensities measured for the untilted pattern.

Since it was deduced from the Patterson-function sections that the Pb atoms in a layer were arranged approximately in hexagonal nets stacked in an $A\ B\ C$ sequence, the structure analysis of the layer was reduced to the problem of finding the deviations from this arrangement consistent with the I_{hk}^0. The contributions of the C and O atoms could be ignored in the initial stages. A series of Fourier projections and difference-Fourier projections led to well-defined Pb positions and ill-defined C and O positions. From these, the I_{hk}^0 and so the C_{hk}^2 were calculated and a new distribution-function Patterson projection was obtained. This was 'idealized' by resolving it into the contributions of sharply-defined vector displacements, and was then used to calculate a new set of C_{hk}^2 and I_{hk}^0. The process was repeated with the alternate calculation of Fourier projections and distribution-function Patterson projections until no further improvement of either was obtained.

The final difference-Fourier projection of the layer structure, from which the Pb contributions have been subtracted, is given in Fig. 2(b). The final distribution function Patterson projection is shown in Fig. 2(c).

In the calculation of structure factors, the phases were found to be dominated by the Pb atom positions. The contributions of the C and O atoms were in no case sufficient to change the sign of A_{hk} or B_{hk}. The positions of the C and O peaks on the difference Fourier projection are thus largely independent of assumed C and O atom positions.

The layer structure

From the evidence of the Fourier projection it was possible to deduce a three-dimensional structure for the layer, i.e. to assign z-parameters for the atoms in such a way that interatomic distances are reasonable and the atomic configurations are chemically sensible. The 'unit cell' for a layer considered by itself is trigonal with space group $P31m-C_3^2$, with $a = b = 9 \cdot 06$ Å, $c = 8 \cdot 27$ Å. The atomic positions relative to this unit cell, including the estimated z coordinates, are given in Table 1. The structure factors for the $hk0$ reflexions, calculated on the basis of the x and y coordinates, are compared with the observed values, corrected for the effect of the distribution function, in Table 2. The value of the discrepancy factor is $R = 0 \cdot 15$.

The composite layer is bounded, top and bottom, by planes of CO_3^{2-} ions. The distance between oxygen atoms at the top of one layer and those at the bottom

Table 1. *Atomic positions*

Kind of atom	Position	Coordinates of typical atom		
		x	y	z
Pb	1(a)	0	0	0·77
	2(b)	⅓	⅔	0·77
	3(c)	0·255±0·005	0	0·50
	3(c)	0·660±0·005	0	0·23
C	1(a)	0	0	0·14
	2(b)	⅓	⅔	0·14
	3(c)	0·66	0	0·86
O^{-2-}	3(c)	0·16	0	0·14
	6(d)	0·53	0·16	0·14
	3(c)	0·51	0	0·86
	6(d)	0·34	0·18	0·86
OH^-	1(a)	0	0	0·42
	2(b)	⅓	⅔	0·42
	3(c)	0·70	0	0·58

Table 2. *Structure factors for hk0 reflexions*

hk	F_c	F_o	hk	F_c	F_o
01	14	16	23	14	11
02	10	13	24	6	7
03	63	62	25	18	19
04	18	13	26	4	4
05	6	7	27	6	5
06	27	25	28	9	11
07	4	4			
08	1	3	33	27	28
09	15	15	34	5	5
			35	5	4
11	12	14	36	15	12
12	20	24	37	6	5
13	7	9			
14	18	19	44	21	22
15	14	8	45	4	4
16	4	4	46	4	4
17	13	16	47	10	4
18	4	6			
			55	13	9
22	28	29	56	4	4

of the next was taken to be 2·8 Å. Between the CO_3^{2-} planes is sandwiched a 'puckered' layer of OH^- ions. Two planes of Pb atoms (designated I and III) in which the Pb atoms are in almost undistorted hexagonal array lie between the CO_3^{2-} planes and the
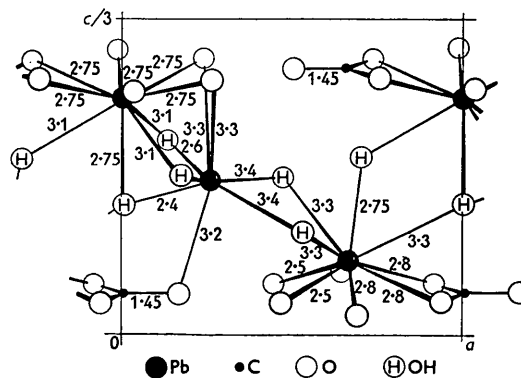

Fig. 3. The arrangement of O^{2-} and OH^- ions around the three Pb atoms in the $y = 0$ plane of the basic lead carbonate layer structure.

OH⁻ layer, but closer to the CO_3^{2-} planes. The other plane of Pb atoms (designated II) lies at the centre of the composite layer and is surrounded by the OH⁻ ions. Fig. 3 shows the surroundings of the three Pb atoms, one in each plane, contained in the $y = 0$ plane of the unit cell. The approximate Pb–O bond lengths are indicated.

The Pb atoms in plane I have surroundings similar to those in the $PbCO_3$ structure. On one side of each Pb atom are six equidistant O atoms, belonging to three CO_3^{2-} groups, with Pb–O distance about 2·75 Å. On the other side, instead of three equidistant O^{2-} ions there are four OH⁻ ions, one directly below the Pb atom at a distance of 2·75 Å and the other three equally spaced at a distance of 3·1 Å. The same arrangement of anions, with slight distortions, surrounds the Pb atom in plane III.

In plane II the Pb atoms are displaced by about 0·8 Å away from the hexagonal net positions towards the Pb atom in plane I at the origin of the x–y projection. The nearest neighbours of these Pb atoms are three OH⁻ ions at distances of 2·4, 2·6 and 2·6 Å, all on the side facing the origin Pb atom.

In the CO_3^{2-} groups, the C–O distance was found to be 1·45 Å, which is considerably greater than the 1·31 Å found, for example, in calcite. Although the accuracy of this determination is limited, the agreement of calculated and observed structure factor was definitely improved by assuming the larger distance.

The stacking of the layers

The initial assumption that the translation between layers was $\pm(\frac{2}{3}, \frac{1}{3})$ was found to be correct only as a first approximation. Subsequent distribution-function Patterson projections, including the final one (Fig. 2(c)), showed very diffuse, roughly triangular peaks around the $\pm(\frac{2}{3}, \frac{1}{3})$ positions, These were interpreted as indicating that the inter-layer translations were slightly different from $\pm(\frac{2}{3}, \frac{1}{3})$, so that the possible translations between nearest-neighbour layers are those indicated by the heavy crosses in Fig. 2(c). Second-nearest neighbour translations are then those indicated by smaller crosses around the $\pm(\frac{2}{3}, \frac{1}{3})$ points. Layers which are third-nearest neighbours, instead of being exactly superimposed, have possible relative translations indicated by the crosses about the origin.

The final distribution-function Patterson projection was idealized, for purposes of calculating layer intensities, by assuming it to be made up of peaks at the positions of the crosses with relative weights as follows:

Weight 24 at (0, 0);

Weight 3 at $\pm[(\frac{1}{3}, \frac{2}{3}) + (0·033, 0·067),$
$(-0·067, -0·033), (0·033, -0·033)]$;

Weight 2 at $\pm[(\frac{1}{3}, \frac{2}{3}) + (0·067, 0·033),$
$(-0·033, -0·067), (-0·033, 0·033)]$;

Weight 1 at $\pm[(\frac{1}{3}, \frac{2}{3}) + (0·067, 0·133),$
$(-0·133, -0·067), (0·067, -0·067)]$;

Weight 1 at $\pm(0·10, 0), (0, 0·10), (-0·10, -0·10)$.

In a disordered crystal it can be assumed that the possible interlayer translations are equally probable, so that, if the $A B C$-type stacking sequence is more or less strictly followed, the average unit cell may be considered to have trigonal symmetry and a c axis of 24·8 Å. If a completely ordered structure were formed, the symmetry would be lower. For example, if the inter-layer translation were always $(\frac{2}{3}, \frac{1}{3}) + (0·067, 0·033)$, or (0·733, 0·367), the unit cell would be triclinic, space group $P1$, with $a = b = 9·06$, $c = 24·8$ Å, $\alpha = 90°$, $\beta = 86° 51'$, $\gamma = 120°$. However, it would seem probable that the energy differences between the various stacking sequences are so small that only in exceptional circumstances could a completely ordered structure be formed.

References

CLARK, G. L. & TYLER, W. P. (1939). J. Amer. Chem. Soc. 61, 58.

COLBY, M. Y. & LACOSTE, L. J. B. (1933). Z. Kristallogr. 84, 299.

COWLEY, J. M. (1953a). Acta Cryst. 6, 516.

COWLEY, J. M. (1953b). Acta Cryst. 6, 522.

COWLEY, J. M. (1956a). Acta Cryst. 9, 397.

COWLEY, J. M. (1956b). Acta Cryst. 9, 399.

COWLEY, J. M. & REES, A. L. G. (1953). J. Sci. Instrum. 30, 33.

FORDHAM, S. & TYSON, J. T. (1937). J. Chem. Soc. p. 483.

GLAUBER, R. & SCHOMAKER, V. (1953). Phys. Rev. 89, 667.

HOERNI, J. A. & IBERS, J. A. (1953). Phys. Rev. 91, 1182.